

# A perturbation approach to predict infrared spectra of small molecular clusters applied to methanol

Udo Buck and Burkhard Schmidt<sup>a)</sup>

Max-Planck-Institut für Strömungsforschung, Bunsenstr. 10, D-3400 Göttingen, Germany

(Received 8 December 1992; accepted 11 March 1993)

A method for predicting splittings and shifts of bands in infrared spectra of small clusters of polyatomic molecules is presented. Based on an approach of early publications of Buckingham, the influence of the intermolecular forces on the vibrational energy levels of the constituent molecules is calculated using perturbation theory to second order. In order to describe the interaction of identical molecules, this *ansatz* is extended to also cover degenerate systems. In first order, a coupling of the vibrational modes of the interacting molecules occurs which leads to delocalized vibrations of all the molecules in the cluster. The second order correction of the vibrational excitation frequencies are found to be dominated by the intramolecular couplings of the normal modes due to the cubic anharmonicity of the force field. The procedures developed here are applied for the interpretation of vibrational photodissociation spectra of small methanol clusters in the region of the fundamental excitation frequency of the OH stretching mode ( $\nu_1$ ,  $3681.5 \text{ cm}^{-1}$ ), the  $\text{CH}_3$  rocking mode ( $\nu_7$ ,  $1074.5 \text{ cm}^{-1}$ ), and the CO stretching mode ( $\nu_8$ ,  $1033.5 \text{ cm}^{-1}$ ). Using semiempirical models for the intermolecular potential functions, splittings and positions of the experimental bands can well be explained. The nonequivalent positions of the two molecules in the linear dimer structure give rise to two different absorption frequencies for each of the three modes of the donor and the acceptor molecule, respectively. The trimer and tetramer spectrum with only one absorption band are in agreement with the existence of symmetric planar ring structures ( $C_{3h}$  and  $C_{4h}$ ) for these species. The pentamer spectrum which also consists of one band is explained by the occurrence of three closely spaced frequencies of an asymmetric ring. The double peak structure in the hexamer spectra can be attributed to a distorted ring structure of  $S_6$  symmetry, while the occurrence of other energetically near-degenerate isomers can be ruled out by means of their spectra.

## I. INTRODUCTION

In recent years, there has been considerable interest in the structure and dynamics of molecular clusters. In particular, great advances in spectroscopic methods have contributed much to the progress in this field. Among the most promising of these techniques are microwave<sup>1</sup> and infrared spectroscopy.<sup>2,3</sup> However, the analysis of the observed spectra may be extremely difficult. Therefore, theory has an important role to play in the investigation of small aggregates and various kinds of computer simulations are now an almost routine tool in the interpretation of cluster spectra.

The special topic of the present publication is the simulation of band shifts observed in vibrational predissociation spectroscopy. In these experiments, a beam of clusters containing infrared-active molecules is formed in a supersonic nozzle expansion into a vacuum chamber. Subsequently, an intramolecular mode of vibration of the constituting molecules is excited by infrared radiation. Relaxation of the energy may then lead to predissociation of the complex which can be monitored as a decrease in the beam signal.<sup>4,5</sup> The spectral bands found in these experiments are shifted with respect to the corresponding gas phase absorption frequencies; sometimes also band split-

tings are observed. The order of magnitude of the frequency shifts lies between several wave numbers ( $\text{cm}^{-1}$ ) for van der Waals systems and a few hundred wave numbers for the X-H vibrations in hydrogen bonded systems. In general, both shifts to higher and lower frequencies (here referred to as blue and red shifts, respectively) may be encountered.

This spectroscopic technique is especially valuable when combined with a method to select the cluster size. Buck and Meyer achieved this by scattering the cluster beam from a second atomic beam in a crossed beam apparatus.<sup>6,7</sup> This method allows to perform spectroscopic or other kinds of experiments on neutral clusters of a single size. The upper limit of the cluster size currently lies at about 15 atoms or molecules.<sup>8</sup> In this manner the vibrational predissociation of a variety of molecular systems has been investigated. They range from van der Waals clusters of  $\text{C}_2\text{H}_4$  (Refs. 9 and 10),  $\text{SF}_6$  (Ref. 11), and  $\text{C}_6\text{H}_6$  (Ref. 12) over strongly polar systems like  $\text{CH}_3\text{CN}$  (Refs. 8 and 13) to hydrogen bonded systems like  $\text{CH}_3\text{OH}$  (Refs. 14–18),  $\text{NH}_3$  (Ref. 19),  $\text{N}_2\text{H}_4$  (Ref. 20), and  $\text{CH}_3\text{NH}_2$  (Ref. 21). For all these systems individual spectra were measured for several different cluster sizes up to the hexamer. Depending on the available laser systems, band shifts of one, two, or three different modes have been observed. In most cases, the spectra obtained for each cluster size are unique and thus contain a large amount of

<sup>a)</sup>Present address: The Fritz Haber Research Center for Molecular Dynamics, The Hebrew University of Jerusalem, Jerusalem 91904, Israel.

information about the cluster geometry and about the underlying intermolecular forces.

In order to fully understand these spectra and to relate them to certain geometrical structures of the molecular aggregates, a method to predict the changes in the characteristic transition frequencies of a molecule is needed. Complete *ab initio* methods including correlation effects<sup>22,23</sup> are only available for dimers of the systems under consideration and are therefore not examined here. Instead we decided to use empirical model functions for the intermolecular potentials and to calculate the influence of the mutual interaction of the molecules on their vibrational spectra. This can be done by means of quantum-mechanical perturbation theory, which has been successfully used over many years in the theory of vibration-rotation spectra of free molecules.<sup>24</sup>

These standard procedures were generalized very early by Buckingham to include the effect of intermolecular forces in a second order formula.<sup>25-27</sup> Similar methods were used to interpret the shifts in electronic spectra of aromatic chromophore molecules in rare gas heteroclusters. For a recent paper we refer to Ref. 28 and the references cited therein. In the spirit of the pioneering work of Buckingham, the pressure dependence of spectra of chromophores in solution<sup>29</sup> as well as frequency shifts of molecules in noble gas matrices<sup>30</sup> could be interpreted. This approach was also applied to the simulation of vibrational spectra of small aggregates of methyl cyanide (CH<sub>3</sub>CN) molecules<sup>31</sup> and to the methanol dimer.<sup>32</sup> However, the frequency shift calculations in all these publications are based on nondegenerate perturbation theory and thus are not directly suited to describe the interaction of identical molecules. In some other work on vibrational band shifts in molecular clusters, degenerate theory was applied in first order only. Moreover, in these contributions the molecular interactions are described by very simple models. The resonant interaction of the transition dipole moments was used to explain the spectra of homogeneous complexes of the highly symmetrical molecules of SF<sub>6</sub>, SiF<sub>4</sub>, and SiH<sub>4</sub> (Refs. 33-36) and of carbon dioxide (Refs. 37 and 38). In a similar manner the shifts of the triply degenerate  $\nu_3$  band of SF<sub>6</sub>-Ar<sub>n</sub> aggregates were attributed to an instantaneous dipole-induced dipole mechanism.<sup>39,40</sup> In another approach vibrational spectra of dimers of SF<sub>6</sub>, SiF<sub>4</sub>, and SiH<sub>4</sub> were calculated to first order using a more realistic potential model.<sup>41</sup> Consequently, there is a clear need for some methodological work to develop new recipes for the calculation of vibrational band shifts. These methods should be based on degenerate perturbation theory to account for the character of the coupled molecular vibrations in the cluster and it should also be possible to include various mechanisms of the molecular interactions.

The methods presented here will be applied to the investigation of spectral line shifts of small methanol clusters. Aside from the water molecule, which has been studied extensively,<sup>42-44</sup> methanol is one of the simplest systems to examine the pattern of hydrogen bonding. One reason for this choice is the availability of intramolecular and intermolecular potential functions in the literature, an-

other reason is rich experimental data obtained with the photodissociation technique described earlier. In the region of the CO stretching mode ( $\nu_8$ , 1033.5 cm<sup>-1</sup>) spectra were measured for size selected clusters ranging from the dimer to the hexamer.<sup>14,15,18</sup> For the dimer spectra of the excitation of the OH stretching mode ( $\nu_1$ , 3681.5 cm<sup>-1</sup>) (Ref. 17) and of the CH<sub>3</sub> rocking mode ( $\nu_7$ , 1074.5 cm<sup>-1</sup>) (Ref. 18) are also available. Most of the measured frequency shifts and splittings are not yet fully understood. Recently, experiments with mixed clusters containing methanol have been published which are beyond the scope of this text.<sup>45</sup>

In the present paper we will also discuss the problem of the occurrence of different isomers. Due to the complexity of the potential hypersurfaces involved, even for systems as small as the clusters investigated here different isomers will be encountered. To attack this problem, the new method to calculate frequencies will be employed. By simulating spectra for various isomers and comparing them to experimental spectra the existence of certain cluster configurations will be confirmed or ruled out.

In the following section the perturbational methods will be described. There we will derive first and second order formulae for the frequency shift using *degenerate* perturbation theory. In Sec. III applications to methanol clusters will illustrate the procedure. After introducing the potential functions used here, the calculated cluster geometries and the corresponding infrared spectra will be presented, compared with experimental results, and discussed.

## II. FREQUENCY SHIFT CALCULATIONS

### A. Perturbation approach for molecular vibrations

The shifts of the characteristic transition frequencies of molecules embedded in a cluster is caused by the fact that the intermolecular binding energy depends on their degree of vibrational excitation. In order to develop a theoretical model for the shifts of vibrational energy levels and the associated band shifts in infrared spectra, we apply the well-known concepts of quantum-mechanical perturbation theory.<sup>46</sup> In this chapter first and second order formulae will be derived using both degenerate and nondegenerate theory. In simulating pure vibrational transitions, only the vibrational energy terms will be considered here, while rotational degrees of freedom are neglected.

A natural starting point is the vibrational Hamiltonian  $H_f$  of the free molecule which can be partitioned into a harmonic part  $H_h$  describing the uncoupled harmonic oscillations and an anharmonic correction  $H_a$

$$H_f = H_h + H_a$$

$$= \frac{1}{2} hc \sum_{r=1}^{3N-6} \omega_r (p_r^2 + q_r^2) + \frac{1}{6} hc \sum_{r,s,t=1}^{3N-6} \varphi_{rst} q_r q_s q_t, \quad (1)$$

where  $\omega_r$  and  $\varphi_{rst}$  are the harmonic frequencies and the cubic force constants in units of wave numbers (cm<sup>-1</sup>), respectively. Higher anharmonic terms are omitted here for reasons of simplicity. The  $q_r$  and  $p_r$  are the position and momentum operators associated with the  $3N-6$  dimen-

sionless normal coordinates of a nonlinear  $N$ -atomic molecule. They are obtained from the standard normal coordinates  $Q_i$  by the conversion

$$q_r = \sqrt{2\pi c \omega_r / \hbar} Q_r. \quad (2)$$

For the perturbation treatment of the anharmonicity, cubic force constants  $\varphi_{rst}$  represented in the basis of (dimensionless) normal coordinates are required. Unlike in the harmonic approximation, it is common practice in anharmonic calculations to take the generally curvilinear character of the internal coordinates into account. Hence, the transformation from internal to normal coordinates is not linear any more. In addition to the  $L$  matrix obtained in a standard normal mode analysis also higher order  $L$  tensors are required. Their elements are calculated using the procedures given by Hoy and co-workers.<sup>47</sup> Based on this representation of the anharmonic force field, vibrational energy levels are routinely calculated by standard formulas treating the cubic anharmonicity  $H_a$  as a perturbation modifying the eigenvalues and eigenfunctions of the harmonic Hamiltonian  $H_h$ .<sup>24</sup> This perturbation approach can be generalized to the situation of molecules in a cluster, liquid, or solid environment. In that case, the effect of the molecular interaction on the vibrational spectra can be described by the Hamiltonian for  $M$  interacting molecules

$$H_c = \sum_{m=1}^M [H_h(m) + H_a(m)] + U. \quad (3)$$

In this equation  $H_h(m)$  and  $H_a(m)$  denote the harmonic and anharmonic part of the intramolecular force field of the  $m$ th molecule and  $U$  stands for the intermolecular interaction energy. This total vibrational Hamiltonian can be split up into an unperturbed Hamiltonian given by

$$H_0 = \sum_{m=1}^M H_h(m) \quad (4)$$

representing the uncoupled harmonic vibrations and into an overall perturbation operator

$$W = \sum_{m=1}^M H_a(m) + U \quad (5)$$

being the sum of the anharmonic components of the intramolecular force fields of the constituting molecules and the interaction potential  $U$ . In general, this potential is a function of both the geometrical arrangement of the molecules and the intramolecular vibrational coordinates. Since the vibrational displacements of the atoms are very small compared to the intermolecular separations, the interaction energy  $U$  may be expanded in powers of these coordinates. Omitting all terms higher than quadratic the potential  $U$  can be written as<sup>25</sup>

$$U = U_0 + \sum_{r=1}^{3N-6} \sum_{m=1}^M \frac{\partial U}{\partial q_{r,m}} q_{r,m} + \frac{1}{2} \sum_{r,s=1}^{3N-6} \sum_{m,n=1}^M \frac{\partial^2 U}{\partial q_{r,m} \partial q_{s,n}} q_{r,m} q_{s,n} + \dots, \quad (6)$$

where  $U_0$  is the interaction energy assuming the molecules to be frozen in their equilibrium position. The dimensionless normal coordinate  $q_{r,m}$  corresponds to the  $r$ th normal mode of the  $m$ th molecule. Note that the derivatives of the intermolecular potential  $U$  are taken keeping all intermolecular degrees of freedom constant. This representation in powers of the  $q_{r,m}$  allows the interaction energy to be treated in a similar manner as the anharmonicity of a free molecule. The perturbing effect of  $W$  on the eigenvalues of  $H_0$  can now be evaluated with standard harmonic oscillator algebra<sup>25</sup> using the simple tabulated formulae for the matrix elements of  $q$ ,  $q^2$ , and  $q^3$ . Once the corrected energy levels of the free molecule and the interacting molecule in a cluster are calculated, the shift of a fundamental excitation frequency can be obtained by

$$\Delta\nu = [(E_1 - E_0)_c - (E_1 - E_0)_f] / (hc) \quad (7)$$

in which the indices  $c$  and  $f$  denote the energy levels of the cluster and the free molecule, respectively. The following sections give the first and second order formulas for the correction of the vibrational ground state  $E_0$  and the first vibrationally excited state  $E_1$  for the molecules in a cluster. These results can be easily generalized to include higher vibrational states.

## B. First order results

Using the harmonic oscillator matrix element  $\langle 0 | q^2 | 0 \rangle = \frac{1}{2}$ , the first order energy correction of the nondegenerate vibrational ground state  $|0\rangle$  of a cluster of  $M$  molecules is given by

$$E_0^{(1)} = \langle 0 | W | 0 \rangle = U_0 + \frac{1}{4} \sum_{r=1}^{3N-6} \sum_{m=1}^M \frac{\partial^2 U}{\partial q_{r,m}^2}, \quad (8)$$

where  $W$  is the perturbation operator introduced in Eq. (5). Note that here and throughout the rest of this text lower indices of  $E$  indicate quantum numbers, while upper indices in angular brackets give the order of perturbation theory. Because only even powers of  $q$  can contribute to the diagonal matrix element of  $W$  required here, there is, in first order, no influence of the cubic anharmonicity on the energy levels or frequency shifts.

Excitation of the fundamental  $a$ th normal mode which is assumed to be nondegenerate renders a system of  $M$  identical molecules in the limit of vanishing interaction in a vibrational state  $E_1$ . To zeroth order, such excited states form an  $M$  fold degenerate manifold. They can be realized by any linear superposition of the form

$$|1_k\rangle = \sum_i b_{ik} |i\rangle. \quad (9)$$

The basis vectors  $|i\rangle$  are defined as states with one quantum in the mode  $q_a$  of the  $i$ th molecule ( $n_a=1$ ) and all other molecules in their vibrational ground states. In order to normalize the wave functions corresponding to the states  $|1_k\rangle$ , it is necessary that the coefficients  $b_{ik}$  defined in Eq. (9) fulfill the condition

$$\sum_i b_{ik}^2 = 1. \quad (10)$$

Under the influence of the molecular interaction potential the energy level  $E_1$  of the states  $|1_k\rangle$  are shifted and split up into  $M$  different sublevels  $E_{1k}$ . In first order perturbation theory these shifts are obtained as eigenvalues of the matrix representation of the perturbation  $W$  in the basis  $|i\rangle$  introduced earlier. The diagonal elements are identical with the first order shifts of the states  $|i\rangle$ , themselves

$$\langle i|W|i\rangle = U_0 + \frac{3}{4} \frac{\partial^2 U}{\partial q_{a,i}^2} + \frac{1}{4} \sum_{r \neq a} \sum_{m \neq i} \frac{\partial^2 U}{\partial q_{r,m}^2} \quad (11)$$

while the strength of the coupling of identical vibrational modes of the molecules is determined by the off-diagonal elements

$$\langle i|W|j\rangle = \frac{1}{2} \frac{\partial^2 U}{\partial q_{a,i} \partial q_{a,j}}, \quad i \neq j. \quad (12)$$

Diagonalization of the energy matrix of the perturbation  $W$  also yields the zeroth order wave functions  $|1_k\rangle$ : The coefficients  $b_{ik}$  defined in Eq. (9) are obtained from the  $k$ th eigenvector of this matrix. They give the vibrational amplitude of the  $i$ th molecule for the respective cluster mode.

The relation (9) characterizing the coupling of the vibrational modes can also be used to give an estimate of the infrared intensities of the excitation of these modes. They are proportional to the square of the corresponding transition dipole moments. They can be obtained in first order by the same type of linear combination

$$\mu(|0\rangle \rightarrow |1_k\rangle) = \sum_i b_{ik} \mu_{a,i} \quad (13)$$

where  $\mu_{a,i}$  stands for the transition dipole moment vector of the  $a$ th normal mode of the  $i$ th molecule. Its absolute value can be deduced from measured intensities of the respective band of the isolated molecule. However, it has to be noted that these infrared absorption intensities cannot be compared directly to intensities observed in vibrational predissociation spectroscopy because the latter ones are also affected by the efficiency of the coupling of the excited states to the continuum of the dissociative states.<sup>48,49</sup>

There are three special cases for which the properties of the first order formulas derived here will have to be discussed more in detail. (1) In the case of symmetrical cluster geometries, it can be shown by group theoretical arguments that the degeneracy of the excited state  $E_1$  may be only partially removed (or not at all). This results in a reduced number of spectral lines, because the eigenvectors  $b_k$  representing the coupled vibrations of the molecules transform according to irreducible representations of the respective symmetry group. Further simplifications of the spectra occur, because, due to the selection rules for infrared spectroscopy, some of the transition moments defined in Eq. (13) vanish. (2) In the case of a heterogeneous cluster where a single chromophore interacts with an environment of atoms or molecules of a different isotopical or chemical species excitation of a nondegenerate mode leads to a nondegenerate state  $E_1$ . Then the first order correction corresponding to this energy level can be calculated by subtracting Eq. (11) from Eq. (8) which leads to a simplified formula for the frequency shift

$$\Delta\nu^{(1)} = E_1^{(1)} - E_0^{(1)} = \frac{1}{2hc} \frac{\partial^2 U}{\partial q_a^2} \quad (14)$$

which is in agreement with the first order result for the frequency shift obtained earlier by Buckingham.<sup>25</sup> It can be interpreted as a direct change in the effective force constant due the intermolecular potential. A positive value of its second derivative leads to an increase in the effective force constant and thus to a blue shift, whereas a negative value results in a red shift. An example for the application of this formula can be found in a publication on the vibrational spectra of ethene-acetone-clusters.<sup>50</sup> (3) It has to be noted that the considerations presented here are only valid for excitations of vibrational modes that are nondegenerate for the free molecule. For the excitation of a  $g$ -fold degenerate vibrational mode the basis  $|i\rangle$  for the representation of the first excited state  $|1_k\rangle$  is of dimension  $g \cdot M$  and the energy matrix defined in Eqs. (11) and (12) has to be extended, accordingly.

### C. Second order results

In the following it is assumed that the perturbing intermolecular potential completely removes the degeneracy of the excited states  $|1_k\rangle$ . Therefore, standard formulae for nondegenerate second order perturbation theory are applied. Making use of simple harmonic oscillator algebra, vibrational energy levels are obtained for each molecule individually. To simplify the calculations, all terms that are independent of the intermolecular potential  $U$  are left out, because their contribution to the shifts of the energy levels  $E_c$  of a molecule in a cluster and to the levels  $E_f$  of a free molecule are identical. Naturally, the omitted terms are the well known second order shifts of the energy levels that are caused by the cubic anharmonicity alone.<sup>24</sup> Neglecting all terms which are quadratic in the second derivatives of the intermolecular potential, one obtains, for this difference,<sup>27</sup>

$$\begin{aligned} \Delta E^{(2)} &= E_c^{(2)} - E_f^{(2)} \\ &= \frac{1}{2} \sum_{r,s} \frac{\varphi_{rrs}}{\omega_s} \frac{\partial U}{\partial q_s} \left( n_r + \frac{1}{2} \right) - \frac{1}{2} \sum_r \frac{1}{hc\omega_r} \left( \frac{\partial U}{\partial q_r} \right)^2. \end{aligned} \quad (15)$$

Inserting the appropriate quantum numbers  $n_r$  for the vibrational ground state  $|0\rangle$  and the first excited state  $|1\rangle$  yields for the second order shift of the fundamental excitation frequency ( $n_r=0 \rightarrow 1$ )

$$\Delta\nu_r^{(2)} = \Delta E_1^{(2)} - \Delta E_0^{(2)} = -\frac{1}{2hc} \sum_s \frac{\varphi_{rrs}}{\omega_s} \frac{\partial U}{\partial q_s}. \quad (16)$$

This formula can be interpreted most easily for the case of a diatomic molecule by identifying the term  $-\partial U/\partial q$  with a force acting along the molecular bond. The cubic force constant  $\varphi$  describing the asymmetry of the intramolecular potential is, typically, strongly negative. Hence, a stretching of the molecule leads to a red shift because the local decrease of the curvature of the bond stretching potential

results in a reduced effective force constant. A decrease of the bond length causes, vice versa, a blue shift of the vibrational band.

For polyatomic molecules, the situation is more complicated, but it may also be explained by the concept of indirect changes of force constants: The summation over all modes  $s$  in Eq. (16) indicates that the generalized forces  $-\partial U/\partial q_s$  corresponding to each of the normal coordinates need to be evaluated. Their contribution to the second order shift of the excitation of the  $r$ th mode are weighted with a factor  $\varphi_{rrs}/2\omega_s$ . The cubic force constant  $\varphi_{rrs}$  describes how the curvature of the intramolecular force field along the normal coordinate  $q_r$  varies linearly with the coordinate  $q_s$ . According to the sign of this constant a force increasing the value of the normal coordinate  $q_s$  results in a red shift ( $\varphi_{rrs} < 0$ ) or in a blue shift ( $\varphi_{rrs} > 0$ ) of the excitation frequency  $\omega_r$ . Therefore, the values of the force constant  $\varphi_{rrs}$  play an important role for the band shift calculations. It has to be noted that for symmetric molecules certain simplifications apply. Using simple group theoretical arguments, it can be shown that the constants  $\varphi_{rrs}$  are only then nonvanishing, if the normal coordinates  $q_s$  transforms like the direct square of the irreducible representation of the coordinate  $q_r$ .<sup>51</sup> This requirement may drastically reduce the number of cubic couplings and thus make the interpretation of the frequency shifts considerably less complex. Once these frequency shifts are obtained for each molecule they are combined to give the correct band shifts of the vibrational modes of the cluster according to Eq. (9).

## D. Discussion

In this section the procedure for band shift calculations proposed in the preceding sections will be critically reviewed. In a comparison with other theoretical treatments of cluster vibrations found in the literature,<sup>52,53</sup> we want to discuss the various levels of approximation and shed some light on the possible applications as well as on certain limitations of the methods developed here.

First, it has to be noted that our frequency shift calculations are based on some early publications of Buckingham.<sup>25-27</sup> His basic idea to treat the intermolecular forces as a quantum mechanical perturbation acting on the vibrations of a molecule that are described in a normal mode approach is adopted here. However, the original work is concerned with the frequency shift in infrared or Raman spectra of chromophores under the influence of a solvent. To account for the disordered structure of a liquid, the resulting band shift formulas have to be averaged over the molecular configurations in a liquid environment. This method can be transferred directly to the theoretical description of (heterogeneous) molecular clusters. In a computer simulation of either bulk matter or small aggregates thermally averaged spectra are obtained by combining the procedure for frequency shift calculations with standard molecular dynamics (MD) or Monte Carlo (MC) techniques. This corresponds to averaging over a microcanonical or a canonical ensemble, respectively. Simulations of

this type will be the subject of a forthcoming paper on methanol clusters.<sup>54</sup>

In many cases, however, small aggregates are known to be rigid at the low temperatures typically found in molecular beam experiments, and the averaging over the configurational space may often be omitted. In principle, the spectra can be calculated for each cluster size and isomer individually. As will be shown in Sec. III, the spectra are remarkably sensitive to the cluster geometry. Therefore, the comparison of theoretical and experimental spectra will contribute considerably to our understanding of intermolecular forces.

In using formulas based on perturbation theory, one must not overlook the general restrictions of such approaches. By definition, their use is limited to very small modifications of the spectra of the free molecules. For vibrational modes involving only heavy atoms, the frequency shifts in van der Waals or hydrogen bonded clusters are typically in the order of  $1-10 \text{ cm}^{-1}$ . In these cases the condition is clearly fulfilled. Perturbation formulas have also been used for the treatment of stretching vibrations of X-H bonds participating in a hydrogen bond where band shifts in the order of a few hundred wave numbers are found.<sup>55</sup> However, care must be taken if the symmetry of the vibrational wave function changes due to the intermolecular binding. As has been demonstrated in a previous study for the example of the water dimer, where the symmetry in the donor molecule is reduced, the Buckingham formula is not adequate in this case.<sup>32</sup>

Another implicit restriction to the general use of Buckingham's approach is that it is based on the harmonic normal mode approximation. Due to the well-known properties of the matrix elements of the harmonic oscillator, the cubic anharmonicity  $\varphi_{rst}$  as well as the first derivatives of the intermolecular potential  $\partial U/\partial q$  do not appear in first order. Therefore it is important to include the second order formula, too. As will be demonstrated later for the example of small methanol clusters, these contributions are not negligible. Of course it is a possible alternative to work with intramolecular potential functions which already include the mechanical anharmonicity. In a study of the solvent shift Dijkman and van der Maas modeled the stretching potential of diatomic molecules using a Morse oscillator.<sup>56</sup> In first order, they obtained a result that is equivalent to Buckingham's second order formula. There are a number of other publications by Watts and co-workers concerned with frequency shifts of the water dimer<sup>57</sup> and of nitrous oxide clusters.<sup>58</sup> Using a local mode approach based on Morse oscillators they applied variational methods instead of the Rayleigh-Schrödinger perturbation theory used here. These methods have not yet been applied for the larger systems investigated here.

It is important to note that there is one fundamental assumption in the work of Buckingham: In treating the vibrations of chromophores interacting with a solvent neighborhood of a chemically different kind, he uses non-degenerate perturbation theory. In order to extend his approach to the theoretical description of the interaction of chemically and isotopically identical molecules, too, gen-

eralized first order formulas based on degenerate perturbation theory are derived in the present work. In this formalism, the excitation of a particular intramolecular vibrational mode cannot be localized in an individual molecule. Instead, the vibrational modes of a cluster are visualized as linear superpositions of the respective modes of the constituting molecules. This concept of delocalized vibrations thus represents an analog to exciton methods used in the theoretical description of optical phonons in molecular solids.<sup>59</sup>

For the reasons given earlier, second order perturbation theory is applied to further increase the accuracy of the calculated frequency shifts. Furthermore, they yield interesting information about the interplay of intramolecular and intermolecular forces as has been shown in greater detail in our previous study on methanol dimers.<sup>32</sup> In the second order treatment given here it is assumed that the perturbing intermolecular potential completely removes the degeneracy of the excited states  $|1_k\rangle$  in first order. This is strictly true only for nonsymmetric cluster configurations, but also for the case of symmetric cluster configurations this is believed to be a reasonable assumption, because even at relatively low temperatures the nonrigidity of the intermolecular bonds leads to a loss of symmetry.

When applying the procedures to a particular system, the most important prerequisite is the detailed knowledge of both the intramolecular and intermolecular potential functions. Special attention must be paid to the dependence of the intermolecular potential on the internal degrees of freedom of the molecules. This information is needed to calculate the derivatives of the type  $\partial U/\partial q$  occurring in the frequency shift formulas in Sec. II. Reliable quantitative models of such a dependence based on a realistic model of the potential energy surface are only available for some atom-molecule systems such as rare gas hydrogen halides.<sup>60</sup> However, a way to circumvent this problem is the use of "site-site" potential models as will be explained in the following chapter for the example of the methanol interaction. It is interesting to note that such an approach already includes the resonant interaction mechanisms in first order: If the electrostatic behavior of the constituting molecules is modeled by partial charges and polarizabilities it can be demonstrated that the leading terms in an expansion of the electrostatic and the induction energy are indeed the dipole-dipole and dipole-induced dipole interactions, respectively.<sup>41</sup> The first of these special approximations has been used to interpret the infrared spectra of homogeneous clusters of the highly symmetrical molecules SF<sub>6</sub>, SiF<sub>4</sub>, and SiH<sub>4</sub>,<sup>33-36</sup> and of CO<sub>2</sub>,<sup>37,38</sup> the second one for the simulation of the spectra of the heterogeneous SF<sub>6</sub>-(Ar)<sub>n</sub> aggregates.<sup>39</sup> Moreover, more complex electrical models including higher order momenta and polarizabilities can be treated in a similar manner.<sup>61</sup> However, it has to be stressed that the method proposed here is far more general in use: it is not restricted to a particular type of interaction, but rather is designed to work with any model of the intermolecular interaction energy.

### III. SMALL METHANOL CLUSTERS

#### A. Intermolecular potential functions

In order to calculate geometrical structures and infrared spectra of molecular clusters, an intermolecular potential function must be known. All the model functions discussed in the following are based on two fundamental assumptions: (1) The total interaction energy of a molecular cluster can be expressed as a sum over all pairs of molecules. Thus, we neglect all three and higher body interactions the most important of which are known to be induction forces.<sup>62</sup> (2) The anisotropy of the underlying pair potentials is described most easily using a "site-site" approximation where each molecule is modeled by a number of sites representing the nuclei and/or electronic charge clouds. Then the interaction of a pair of molecules is taken to be the sum of the pairwise contributions of all sites on either molecule. Note that this assumption implicitly also gives a simple model for the stretching and bending dependence of the intermolecular binding energy. Derivatives of the interaction energy with respect to vibrational coordinates occurring in the line shift formulae presented in Sec. II can be obtained by simply displacing the atomic sites along the normal modes of vibration.

For the methanol calculations we chose two different empirical potential functions, the optimized potentials for liquid simulations (OPLS) model of Jorgensen<sup>63</sup> and a model published by Pálinkás *et al.* which will be referred to as PHH3.<sup>64</sup> They were obtained by comparing experiments and simulations of condensed phase systems. In both cases, the methanol interaction is described by three potential sites (CH<sub>3</sub>, O, and H). The corresponding partial charges yield an electrostatic dipole moment of  $7.4 \times 10^{-30}$  and  $6.4 \times 10^{-30}$  Cm, respectively.<sup>65</sup> Note that the first one overestimates the experimental value by about 25% to account for the nonadditivity and the induction forces missing in the simple model. For this potential, the value of the transition dipole moment of the CO stretching mode  $\nu_8$  of  $0.82 \times 10^{-30}$  Cm is in remarkably good agreement with experimental results obtained from Rabi oscillations in Stark spectra.<sup>66</sup> The nonelectrostatic parts of the interaction are modeled in two different ways: In the OPLS potential, there are Lennard-Jones 12-6 potentials only for the CH<sub>3</sub> and O sites. In the PHH3 potential, sophisticated Morse-type functions are used to model the O and H interactions in a more realistic way, while the remaining interactions are constructed using the same functions and parameters as in the OPLS potential.

Two other potentials considered here are the empirical potentials based on electrons and nuclei (EPEN/2)<sup>67</sup> and the quantum mechanical potentials based on electrons and nuclei (QPEN) model.<sup>68</sup> Both models involve potential sites representing binding and lone pair electrons which results in a total number of 14 sites. This leads to additional difficulties in the theoretical description of the vibration dependence of the interaction energy. Therefore, we decided not to use them for the simulations of spectral line shifts presented in the following.

As a first simple check of the various methanol poten-

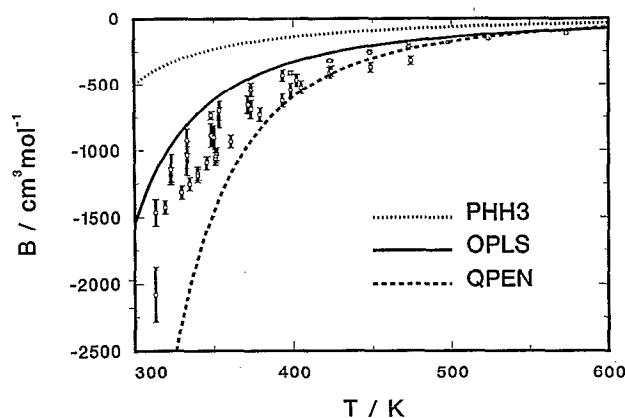


FIG. 1. Second virial coefficients of methanol vapor. The open squares with error bars indicate experimental values taken from Ref. 71. The curves show the values calculated for three different potential models mentioned in the text.

tial models presented above, we inspected the temperature dependence of the second virial coefficients of methanol vapor. Employing a nonproduct integration scheme proposed by Evans and Watts, the values of  $B(T)$  were calculated using approximately  $10^6$  integration points.<sup>69,70</sup> Figure 1 shows a comparison with experimental values compiled by Dymond and Smith.<sup>71</sup> Only the virial coefficients obtained for the OPLS potential are in satisfactory agreement with the experimental ones, while for the other potentials there are major discrepancies in the low temperature region indicating a too low and a too high estimation of the hydrogen bond strength in the PHH3 and the QPEN potential models, respectively.

## B. Cluster geometries

Using the empirical potential models introduced earlier, stable cluster geometries and the respective binding energies are searched for. For these calculations, the constituting molecules are kept rigid in their equilibrium configurations. The position and orientation of each molecule are represented by three Cartesian coordinates defining the center of mass and by three Euler angles of rotation. Starting from randomly chosen configurations, these intermolecular degrees of freedom are optimized without constraints in order to find local minima of the potential energy hypersurface. Out of a variety of different algorithms tested, a Newton-like strategy is found to perform most efficiently.<sup>72</sup> To find the most stable isomer of the methanol hexamer, a typical number of several hundred minimization runs is necessary to ensure that the global minimum has been found.

The results of these minimizations are summarized in Table I for cluster sizes ranging from the dimer to the hexamer. The potential well depths and the symmetry groups of the most stable isomers are listed. The binding energies for the OPLS potential are generally about 20% larger than for the PHH3 potential. Given the mainly electrostatic character of the hydrogen bond, this discrepancy can be attributed to the different dipole moments for these

TABLE I. Binding energies (in kJ/mol) and symmetry groups of small methanol clusters as a function of the cluster size  $M$ . The first columns give the most stable isomers found using two semiempirical potential models [OPLS (Ref. 63) and PHH3 (Ref. 64)], the last column gives results from *ab initio* calculations (Ref. 73).

$M$	OPLS		PHH3		STO-3G
	$\Delta E$	Symm.	$\Delta E$	Symm.	$\Delta E$
2	-28.53		-23.44		-23.4
3	-73.44	$C_{3h}$	-59.18	$C_{3h}$	-64.0
4	-124.78	$C_{4h}$	-98.38	$S_4$	-147.6
5	-166.19		-132.44		-201.9
6	-204.13	$S_6$	-162.27	$S_6$	-248.7

potential models. The results obtained for the empirical potential functions can be contrasted with self-consistent field (SCF) calculations<sup>73</sup> that are also given in Table I. The comparison shows that the PHH3 potential gives a reasonable estimate for the bond strength of the dimer ( $\Delta E = -23.44$  kJ/mol). This value is also in good agreement with experimental and theoretical work by Bizzarri *et al.*<sup>74</sup> However, using this potential model, one slightly underestimates the total binding energy of the larger clusters. On the other hand, the dimer binding energy of  $\Delta E = -28.53$  kJ/mol obtained for the OPLS potential is clearly too large, while the values for the larger clusters are more realistic. In this context it is instructive to calculate the incremental binding energy  $\Delta E_M - \Delta E_{M-1}$  as a function of the cluster size  $M$  as shown in Fig. 2. Due to the cooperativity of hydrogen bonds, the *ab initio* results show a pronounced maximum of this function for the tetramer ( $M = 4$ ). This is in good agreement with measurements of thermodynamical properties of the gas phase indicating a particularly high stability of this species.<sup>75,76</sup> Although the empirical potentials used here do not explicitly account for the nonadditivity of the methanol interactions, they are able to reproduce the behavior of this function qualitatively.

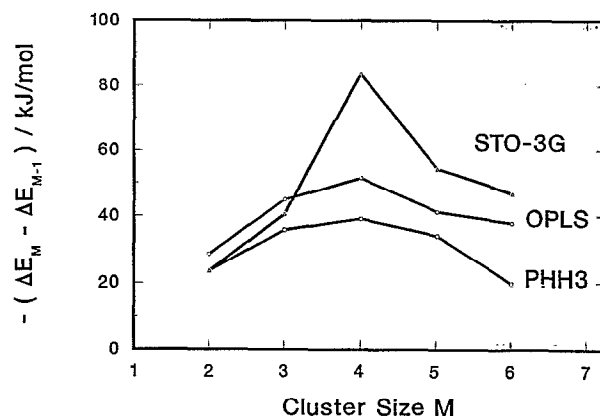


FIG. 2. Incremental binding energies of small methanol clusters. The open circles and the open squares give the values obtained for the empirical OPLS and PHH3 potential models, respectively. The open triangles show results of *ab initio* calculations (Ref. 73).



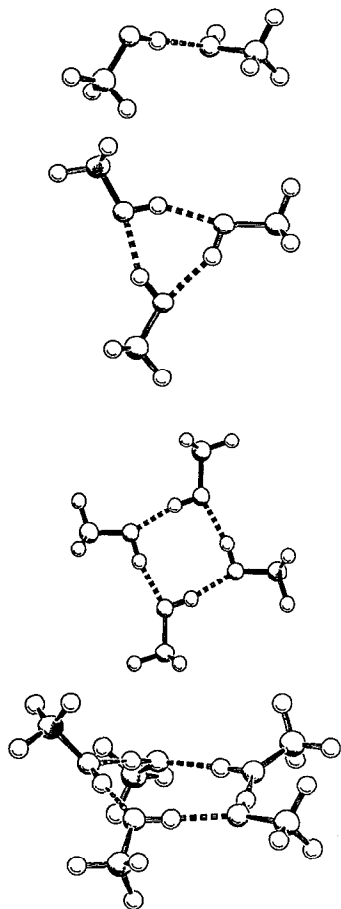


FIG. 3. Dimer, trimer, tetramer, and pentamer structures of methanol. The geometrical structures represent the most stable isomers obtained using the OPLS potential. The corresponding binding energies are given in Table I.

In Figs. 3 and 4 some examples of the corresponding cluster geometries are depicted. As in the case of the water dimer, the dimer is characterized by a linear O—H—O hydrogen bond (see Fig. 3) with an O—O distance of 274 and 285 pm for the OPLS and the PHH3 potential, respectively. Regardless of the potential model used, the energetically most favored forms for all other cluster sizes investigated here are found to be rings with a coordination number of 2. Although there are considerable deviations from the linear H-bond geometry which has been found for the dimer, the ring strain is compensated for by one additional hydrogen bond. This is in good agreement with other theoretical and experimental work on these systems. Using the QPEN potential, Martin *et al.* predicted rings to be the most stable forms for clusters of up to ten molecules.<sup>77</sup> In another study, Brink and Glasser also found cyclic trimer and tetramer structures for the EPEN potential.<sup>78</sup> The only direct experimental evidence on the structure of small methanol aggregates are measurements of molecular beam deflection in inhomogeneous electrical fields.<sup>79</sup> The dimer was found to be polar, while for the other small clusters an upper limit for the electrostatic dipole moment of only  $10^{-30}$  Cm could be established. This suggests a linear structure for the dimer and relatively

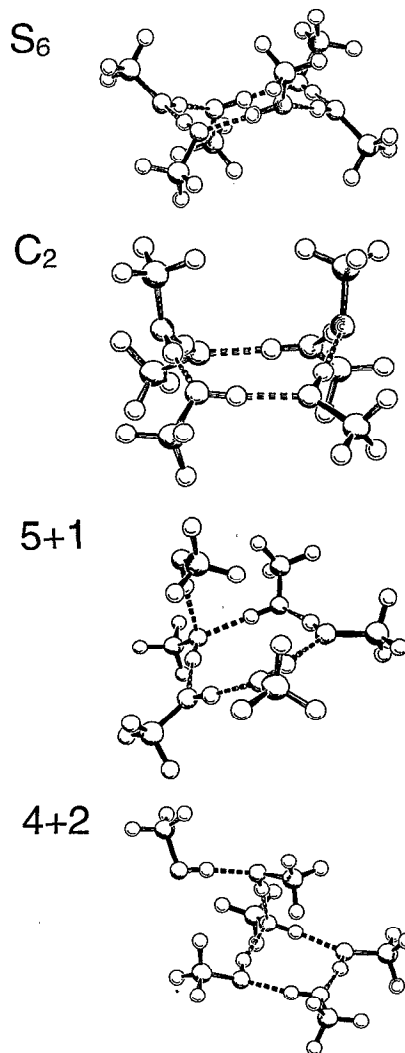


FIG. 4. Structures of four different isomers of the methanol hexamer found for the OPLS potential. They are referred to as  $S_6$ ,  $C_2$ , 5+1, and 4+2 (from the top to the bottom). The binding energies are  $-204.13$  kJ/mol,  $-203.47$  kJ/mol,  $-197.64$  kJ/mol, and  $-191.23$  kJ/mol, respectively.

planar ring structures for the remaining clusters.

The only difference in the cluster geometries predicted for the various potential models is the symmetry of the ring structures. Below a certain upper limit of the cluster size, the most stable isomers are planar with a  $C_{Mh}$  symmetry for an aggregate of  $M$  molecules. For larger systems the rings start to be distorted. For an odd number of molecules this leads to asymmetrical configurations, while even number clusters prefer an  $S_M$  symmetry with a simple alternation of the methyl groups above and below the plane of the ring. The trimer and tetramer structures obtained with the OPLS potential are planar with  $C_{3h}$  and  $C_{4h}$  symmetry and binding energies of  $\Delta E = -73.44$  kJ/mol and  $\Delta E = -124.78$  kJ/mol, respectively (see Fig. 3). Using this potential model, the pentamer is the first cluster to deviate from strict planarity ( $\Delta E = -166.19$  kJ/mol). The geometry of this distorted ring can also be seen in Fig. 3. This situation is contrasted with the results for the PHH3 po-



tential where only the trimer is planar ( $C_{3h}$ ), but already for the tetramer a slightly nonplanar ring of  $S_4$  symmetry is found. For the EPEN/2 potential already the most stable trimer structure is slightly distorted. However, its dipole moment of  $0.9 \times 10^{-30}$  Cm is still below the upper limit obtained from the results of the beam deflection experiments mentioned earlier.<sup>79</sup>

Up to the pentamer there are no other isomers energetically close to the ring structures discussed so far. The energetically lowest chainlike structures are considerably less stable. For example, using the OPLS potential a difference in the binding energies of 10.6 and 23.3 kJ/mol is obtained for the trimer and tetramer, respectively. Therefore, for the interpretation of spectroscopic experiments with molecular beams, these isomers need not be considered. The situation is, however, completely different for the hexamer. A thorough investigation of the OPLS potential hypersurface yields (at least) four different classes of isomers for this system. They are shown in Fig. 4. The two most stable configurations of the hexamer are distorted hexagonal ring structures of different symmetry. The energetically lowest one ( $\Delta E = -204.13$  kJ/mol) is a ring of  $S_6$  symmetry followed by another ring of much lower symmetry ( $C_2$ ) which is only slightly less stable ( $\Delta E = -203.47$  kJ/mol). These structures resemble the well-known "seat" and "boat" isomers of the cyclohexane molecule. The former geometry was also proposed for the water hexamer.<sup>80,81</sup> It is noted that this isomer was overlooked in our first calculations in Ref. 14(b). Aside from this nearly degenerate pair of isomers, other classes of cluster geometries consisting of branched rings are encountered. We find a ring of five molecules with an attached monomer ( $\Delta E = -197.64$  kJ/mol) and a ring of four molecules with an attached dimer unit ( $\Delta E = -191.23$  kJ/mol).

### C. Intramolecular force fields

In order to calculate second order frequency shifts, an intramolecular force field must be known that accounts at least for the most important contributions to the anharmonic coupling of the twelve vibrational normal modes of the methanol molecule. In principle, these data can be obtained from a fit to experimental spectra, but because of the large number of parameters this method is usually limited to di- and triatomic molecules.

Instead, we choose a force field determined by *ab initio* SCF calculations with a standard 4-31G basis set published by Schlegel and co-workers.<sup>82</sup> This intramolecular potential is represented in nonsymmetrized valence coordinates and it includes all cubic force constants of the form  $F_{ijj}$  as well as the quartic force constants  $F_{iiii}$  for the bond stretching coordinates. Although the anharmonic frequencies obtained with this model are generally slightly higher than the corresponding experimental values, we decided not to scale the force constants, because the absolute values of these constants are not important for band shift calculations.

For the perturbation treatment of the anharmonicity and of the intermolecular interaction, the cubic component of the force field needs to be represented in the basis of

(dimensionless) normal coordinates. This is provided by carrying out a nonlinear transformation from internal to normal coordinates using higher order  $L$  tensors according to the methods given by Hoy *et al.*<sup>47</sup> When inspecting the results of this transformation, we want to focus our attention on the force constants  $\varphi_{77s}$  and  $\varphi_{88s}$  playing an important role for the calculation of the  $\nu_7$  and  $\nu_8$  band shift in methanol clusters. The diagonal constants  $\varphi_{777}$  and  $\varphi_{888}$  are strongly negative ( $-132$  and  $-279$   $\text{cm}^{-1}$ ). Furthermore, there are some large off-diagonal constants. Because the  $\nu_7$  mode ( $\text{CH}_3$  rock) and  $\nu_8$  mode (CO stretch) transform like the totally symmetric irreducible representation ( $A'$ ) only the cubic couplings  $\varphi_{88s}$  with  $s$  being another  $A'$  mode are nonvanishing. Especially the cubic coupling to the  $\nu_1$  mode (OH stretching) is strikingly large with  $\varphi_{771} = +249$   $\text{cm}^{-1}$  and  $\varphi_{881} = +253$   $\text{cm}^{-1}$ . Since this number plays an important role in the interpretation of the band shifts,<sup>32</sup> it is worthwhile to compare it to the values obtained from other data. Botschwina *et al.* investigated the force fields of some small OH compounds using SCF methods, also.<sup>83</sup> The aforementioned nonlinear transformation of the force constants yields the value of  $\varphi_{881} = +105$   $\text{cm}^{-1}$  for the cubic coupling of the CO stretching mode and the OH stretching mode. Although there is no quantitative agreement, these calculations confirm the trend of a large positive coupling constant. To obtain a more precise cubic force field, *ab initio* calculations beyond SCF level are desirable.

### D. Infrared spectra

In this chapter band shifts will be calculated for small methanol clusters. We restrict ourselves to the most stable configurations obtained with the empirical potentials. The numbers given in the text refer to the OPLS model. The final results, however, are also calculated for the PHH3 potential and are presented later when the results of all the frequency shift calculations are summarized. Our special focus will be on the fundamental excitation band of the CO stretching mode  $\nu_8$ . For gaseous methanol this frequency lies at  $1033.5$   $\text{cm}^{-1}$ .<sup>84</sup> For small methanol aggregates with cluster sizes ranging from  $M=2$  to  $M=6$  band splittings and shifts in the order of  $10$   $\text{cm}^{-1}$  to either side were detected in vibrational predissociation spectra of size selected clusters.<sup>14</sup> For the dimer also measurements in the region of the OH stretching mode ( $\nu_1$ ,  $3681.5$   $\text{cm}^{-1}$ ) and of the  $\text{CH}_3$  rocking mode ( $\nu_7$ ,  $1074.5$   $\text{cm}^{-1}$ ) were carried out.<sup>17,18</sup> The frequency shift of the  $\nu_1$  mode is much larger, while the shift of the  $\nu_7$  mode is of the same order of magnitude as those found for the  $\nu_8$  mode. Table II gives a summary of the first and second order contributions to the frequency shifts of the three modes of vibration for the methanol dimer obtained with the OPLS potential.

First, the  $\nu_8$  band shift is calculated in first order for the asymmetric methanol dimer structure shown in Fig. 3. Using the nondegenerate formalism of Eq. (14) the resulting values for  $(1/2)\partial^2 U/\partial q_8^2$  are  $+10.2$  and  $+5.6$   $\text{cm}^{-1}$  for the proton donor and acceptor molecule, respectively. These blue shifts can be explained by an increase in the effective force constant of the  $\nu_8$  mode caused by the hy-

TABLE II. First and second order contributions to the band shifts  $\Delta\nu$  (in  $\text{cm}^{-1}$ ) for the methanol dimer using the OPLS potential. The band centers of the respective gas phase absorption lie at  $3681.5 \text{ cm}^{-1}$  ( $\nu_1$ , OH stretch), at  $1074.5 \text{ cm}^{-1}$  ( $\nu_7$ ,  $\text{CH}_3$  rock), and at  $1033.5 \text{ cm}^{-1}$  ( $\nu_8$ , CO stretch). The last two lines of the table give the vibrational amplitudes  $b_{ik}$  of the donor and acceptor molecule defined in Eq. (9).

Mode	$\Delta\nu_1$		$\Delta\nu_7$		$\Delta\nu_8$	
First order <sup>a</sup>	+6.2	-36.9	+26.5	-0.5	+12.9	+3.0
Second order <sup>b</sup>	+14.4	-202.5	+10.5	-3.1	+16.0	-1.6
Total	+20.6	-239.4	+37.0	-3.6	+28.9	+1.3
$b_{ik}$ (donor)	-0.27	+0.96	+1.00	+0.01	+0.86	+0.52
$b_{ik}$ (acceptor)	+0.96	+0.27	-0.01	+1.00	-0.52	+0.86

<sup>a</sup>See Eqs. (8)–(12).

<sup>b</sup>See Eq. (16).

drogen bond. This effect is much stronger in the donor, because of some contributions of the COH bending motion to the  $\nu_8$  mode which are strongly hindered.

In the formalism of degenerate perturbation theory the energy matrix has to be set up. Aside from the pure second derivatives of the potential energy  $U$  occurring in the diagonal elements of Eq. (11), also the mixed second derivative has to be calculated. The resulting off-diagonal element of the energy matrix in Eq. (12) of  $-4.4 \text{ cm}^{-1}$  (OPLS) has important consequences. Apart from further increasing the distance of the vibrational bands which are now shifted by  $+12.9$  and  $+3.0 \text{ cm}^{-1}$  with respect to the gas phase absorption frequency, it also causes a coupling of the  $\nu_8$  vibrations of either molecule. Therefore, the vibrational modes of the dimer cannot be localized in the individual molecules any more. Instead they can be described by linear superpositions of the single molecule vibrations as given in Eq. (9). For the dimer the absolute values of the respective coefficients  $b_{ik}$  are 0.855 and 0.518. The upper of the two sublevels is mostly a donor vibration with some admixture of acceptor vibration, while the situation is reversed for the lower of the two states. In the first case, the two CO oscillators are vibrating out of phase, while in the second case they are vibrating in phase. It is noted that, due to the difference of the coefficients, the picture of non-degenerate perturbation theory which was used in a previous study is still a relatively good approximation in this particular case.<sup>32</sup>

In second order, further corrections of the frequency shifts are calculated. In a first step this is done for the two molecules individually. As has been shown in greater detail in our earlier study and can be seen in Eq. (16), the cubic anharmonicity of the intramolecular force field plays a notable role.<sup>32</sup> The most important contributions to the second order shifts are explained in the following for the example of the OPLS potential: (1) The intermolecular forces give rise to an increase of the CO bond length. Because of the asymmetry of the CO stretching potential this results in a decrease of the fundamental transition frequency. This shift of  $-13.5$  and  $-16.8 \text{ cm}^{-1}$  for the donor and the acceptor molecule, respectively, is approximately the same for the two molecules. (2) In the donor molecule there is a strong force stretching the OH bond. With the large positive cubic force constant  $\varphi_{881} = +253 \text{ cm}^{-1}$  this

leads to a remarkable blue shift of the  $\nu_8$  excitation frequency of  $+18.6 \text{ cm}^{-1}$ . It is this coupling of the OH and the CO stretching mode that mainly causes the difference in the second order shifts of the two nonequivalent molecules. In total, they are  $+12.9$  and  $-9.7 \text{ cm}^{-1}$  for the donor and the acceptor molecule in each case. In the next step the second order shifts for the coupled vibrational modes of the methanol dimer are obtained by weighting these values with the coefficients  $b_{ik}$  according to Eq. (9). This gives  $+16.0 \text{ cm}^{-1}$  for the higher frequency excitation and  $-1.6 \text{ cm}^{-1}$  for the lower one thus yielding total band shifts of  $+28.9$  and  $+1.3 \text{ cm}^{-1}$  for the two modes.

The interpretation of the  $\nu_1$  band shifts is less complicated. Here, the first order coupling induced by the off-diagonal elements of the energy matrix given in Eq. (12) is very small. The two modes of the dimer vibration essentially are identical to the OH stretching vibrations of the donor and the acceptor molecule alone. Hence, the first order shifts can be calculated according to Eq. (14) and interpreted in the simple picture of a direct force constant change. The shifts of  $+6.2$  and  $-39.2 \text{ cm}^{-1}$  can be attributed to an increase of the OH stretching force constant in the acceptor and a decrease of this constant in the donor, respectively. In the latter molecule, however, the most important contribution to the total  $\nu_1$  frequency shift is an indirect change of the force constant. The forces increasing the OH bond length cause an additional red shift of  $-202.5 \text{ cm}^{-1}$ . The cubic couplings to other  $A'$  modes are of no importance here.

Although the  $\nu_7$  mode of the methanol molecule is commonly referred to as  $\text{CH}_3$  rocking vibration,<sup>34</sup> one has to be aware that there is also a strong admixture of a COH bending motion. This contribution is mostly responsible for the  $\nu_7$  band shifts occurring in clusters, while the  $\text{CH}_3$  rocking motion is hardly influenced by the hydrogen bonding. Again there is no intermolecular coupling of the modes in the dimer, i.e., the two vibrational modes can be localized in either one of the molecules. The excitation frequency of the acceptor molecule is only slightly changed ( $\Delta\nu_7 = -3.6 \text{ cm}^{-1}$ ), but there is a pronounced shift for the donor molecule. The first order shift of  $+26.5 \text{ cm}^{-1}$  is caused by a hindering of the COH bending motion. To second order the strong coupling to the OH stretching

TABLE III. Theoretical and experimental band shifts  $\Delta\nu$  (in  $\text{cm}^{-1}$ ) of small methanol clusters of size  $M$ . The calculated values refer to the most stable isomers specified in Table I and are obtained for the OPLS and PHH3 potential. Note that only the infrared active modes are included. The respective irreducible representations are given in the last column. For comparison, experimental values obtained from vibrational predissociation spectra are also listed (see text).

$M$	mode	OPLS	PHH3	Experiments	Remarks
2	$\Delta\nu_1$	+20.6	+70.3	+1	mostly acceptor
	$\Delta\nu_1$	-239.4	-145.1	-107	mostly donor
	$\Delta\nu_7$	+37.0	+25.2	...	donor
	$\Delta\nu_7$	-3.6	-2.1	-3	acceptor
	$\Delta\nu_8$	+28.9	+24.2	+18	mostly donor
3	$\Delta\nu_8$	+1.3	-1.7	-7	mostly acceptor
	$\Delta\nu_8$	+3.8	+64.3	+8	$E'$
4	$\Delta\nu_8$	+24.9	+26.6	+10	$E_u/E$
5	$\Delta\nu_8$	+27.5	+16.9		
	$\Delta\nu_8$	+21.0	+16.6	+14	
	$\Delta\nu_8$	+17.2	+14.7		
6	$\Delta\nu_8$	+32.8	+22.9	+18	$A_u$
	$\Delta\nu_8$	+17.0	+9.8	+6	$E_u$

mode ( $\varphi_{771} = +249 \text{ cm}^{-1}$ ) leads to an additional blue shift of  $+10.5 \text{ cm}^{-1}$ .

For the OPLS potential, the energetically lowest isomers of the trimer and the tetramer are planar rings of  $C_{3h}$  and  $C_{4h}$  symmetry. For these clusters the approximation of modes that are associated with the vibrations of single molecules does not hold any more. Instead we are dealing with highly coupled and thus delocalized vibrational modes. Therefore, it is essential to use the degenerate perturbation formulae given in Eqs. (9)–(12). Application of simple group theoretical arguments simplifies the interpretation of the infrared spectra considerably. The first excited state of the trimer is split up into a single ( $A'$ ) and into a twofold degenerate ( $E'$ ) level. For the tetramer there are one  $A_g$ , one  $B_g$  and one  $E_u$  representation. In each case the levels transforming like the totally symmetric representations  $A'$  and  $A_g$ , respectively, correspond to cluster vibrations for which all the molecules are vibrating in phase. Since the vector sums of the transition dipole moments defined in Eq. (13) vanish, these modes cannot be excited by infrared radiation. This is also true for the  $B_g$  mode of the tetramer, where opposite molecules vibrate pairwise in phase. Hence, only the states of the  $E'$  and  $E_u$  symmetry can be excited in the trimer and tetramer, respectively. From this statement it follows that there is only one doubly degenerate band in the region of each fundamental excitation frequency. The respective first order  $\nu_8$  frequencies are shifted to the blue by  $+3.8 \text{ cm}^{-1}$  for the trimer and by  $+24.9 \text{ cm}^{-1}$  for the tetramer. Due to the symmetry, there are no second order shifts. Note, however, that the situation is different for the nonplanar tetramer structure of  $S_4$  symmetry found for the PHH3 potential model. There, the representation of the four molecules can be reduced into  $A+B+E$ . Hence, the excitation spectra for this species consist of one single ( $B$ ) and one twofold degenerate ( $E$ ) band. However, because of the near planarity of this cluster configuration, the intensity of the  $B$  mode is much lower than that of the  $E$  mode. Therefore, this mode has not been included in the

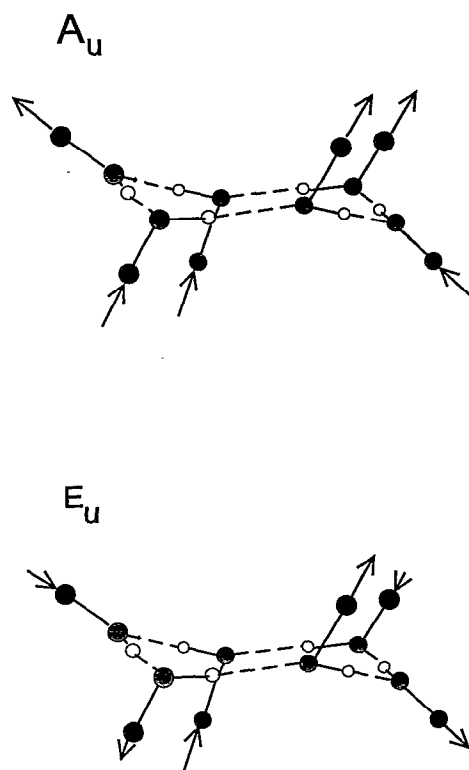


FIG. 5. Infrared active modes of the methanol hexamer of  $S_6$ -symmetry. The arrows mark the relative amplitudes of the CO stretching vibrations according to the coefficients  $b_{ik}$  given in Eq. (9). Upper: the  $A_u$  mode. Lower: the  $E_u$  mode.

comparison of the data shown in Table III.

For the asymmetric structures of the methanol pentamer, the characteristic frequencies are split into five bands. For two out of the five modes of the  $\nu_8$  excitation, however, the intensity given by the squared transition dipole moment is about 1 order of magnitude smaller than for the remaining ones. Hence, the respective spectra can be approximately represented by the three bands given in Table III. They are shifted towards higher frequencies by  $+27.5$ ,  $+21.0$ , and  $+17.2 \text{ cm}^{-1}$ .

The interpretation of the hexamer spectrum is particularly interesting because of the occurrence of the energetically near-degenerate isomers as is depicted in Fig. 4. For the energetically lowest configuration of the hexamer, the spectrum is mainly determined by the  $S_6$  symmetry of this isomer. In this case, the representation of the first excited state reduces to  $A_g + E_g + A_u + E_u$ . Like for the other symmetric ring structures discussed above, the totally symmetric cluster mode ( $A_g$ ) does not contribute to the infrared spectrum. Analogously to the  $B$  modes of the tetramer, there are also coupled vibrational modes where opposite molecules vibrate pairwise in phase. These modes transform like the  $E_g$  representation and are not infrared active. The remaining modes are  $A_u$  and  $E_u$ , thus the predicted spectrum has one single and one doubly degenerate vibrational band in the region of the  $\nu_8$  excitation frequency. Their shifts with respect to the monomer absorption amount to  $+32.8$  and  $+17.0 \text{ cm}^{-1}$ . The coupling scheme

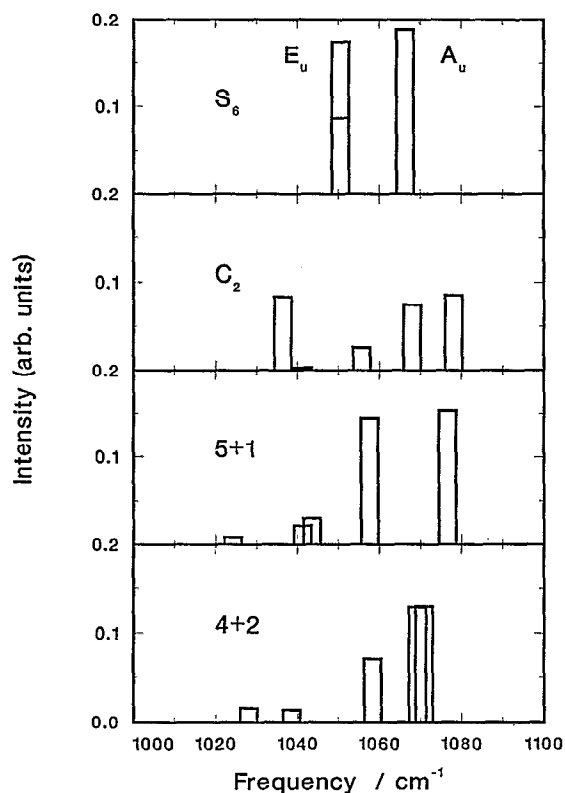


FIG. 6. Calculated infrared spectra in the region of the  $\nu_8$  excitation frequency ( $1033.5 \text{ cm}^{-1}$ ). Using the perturbational scheme of this work, frequency shifts are calculated for the four different isomers of the methanol hexamer found for the OPLS potential. They refer to the geometrical configurations in Fig. 4. Note that absorption frequencies occur outside the plotted region ( $1000\text{--}1100 \text{ cm}^{-1}$ ). The height in the stick spectra represents the relative infrared intensity calculated as the square of the transition dipole moment given in Eq. (13).

of the vibrations of the molecules for these two modes of the cluster vibration is shown in Fig. 5.

The remaining isomers found for the methanol hexamer exhibit fundamentally different spectra: For the other six-membered ring structure of  $C_2$  symmetry which is only slightly less stable the first vibrationally excited state can be decomposed into  $3A + 3B$ . Hence, there are no simplifications of the infrared spectrum which consists of six lines. The same is also true for the other classes of non-symmetric isomers consisting of branched rings. Calculated stick spectra of the four isomers in the region between  $1000$  and  $1100 \text{ cm}^{-1}$  are displayed in Fig. 6.

## E. Discussion

In what follows we want to discuss our calculated results for the band shifts in small methanol clusters up to the hexamer. The theoretical values obtained for both the OPLS and the PHH3 potential models always refer to the respective most stable cluster geometries as listed in Table I and illustrated in Figs. 3 and 4. For comparison with experimental spectra, a selection of data is necessary: For the  $\nu_1$ ,  $\nu_7$ , and  $\nu_8$  mode of the dimer we chose the results from experiments of Huisken *et al.*<sup>15,17,18</sup> which for the  $\nu_8$  mode are essentially in coincidence with the measurements

by Lacosse and Lisy.<sup>16</sup> For spectra in the region of the  $\nu_8$  mode excitation of larger clusters we refer to the results of Buck and co-workers which are at present available for cluster sizes up to the hexamer.<sup>14</sup> Experimental spectra in the region of the other modes are not available for size selected clusters. A compilation of the theoretical and experimental frequency shifts is given in Table III.

First of all, when interpreting the experimental spectra the number and assignment of the bands will be of some interest. Making use of simple group theoretical arguments the number and degree of degeneracy alone can give valuable hints about the geometry of the cluster under investigation. In the experimental spectrum of the methanol dimer there are two features in the region of the  $\nu_1$  excitation band. Compared with the monomer absorption at  $3681.5 \text{ cm}^{-1}$ , one of them is essentially unchanged ( $\Delta\nu_1 = +1 \text{ cm}^{-1}$ ), while the other one is shifted far towards the red ( $\Delta\nu_1 = -107 \text{ cm}^{-1}$ ). Close to the fundamental  $\nu_8$  excitation frequency at  $1033.5 \text{ cm}^{-1}$  there are two bands in the photodissociation spectra, one is shifted to the blue ( $\Delta\nu_8 = +18 \text{ cm}^{-1}$ ), the other one to the red ( $\Delta\nu_8 = -7 \text{ cm}^{-1}$ ). This splitting of the  $\nu_1$  and  $\nu_8$  frequencies can be easily explained with a linear dimer structure and the nonequivalent positions of the donor and the acceptor molecule. The red shifted component of the  $\nu_1$  band is due to the absorption of the donor molecule while the unshifted one is caused by the acceptor absorption. Aside from these rather evident findings, also the spectra in the region of the  $\nu_8$  band can be explained. Our calculations show that the blue shifted band can be attributed to the excitation of a vibrational mode of the dimer that is mostly located in the donor, while the other one is mainly an acceptor vibration. This is in agreement with results obtained from liquid spectroscopy. Studying the spectra of methanol under the influence of various solvents, Kabisch and Pollmer concluded that the CO stretching frequency of a methanol molecule increases, if hydrogen bonding occurs through its hydroxyl H atom, while it decreases, if the molecule acts as an acceptor.<sup>85</sup> Moreover, the values for the shifts of  $+13$  and  $-4 \text{ cm}^{-1}$  are similar to the experimental results for gas phase dimers which are  $+18$  and  $-7 \text{ cm}^{-1}$ . In the region of the  $\nu_7$  excitation at  $1074.5 \text{ cm}^{-1}$  only one slightly red shifted band was found ( $\Delta\nu_7 = -3 \text{ cm}^{-1}$ ). In the present work this is attributed to the absorption of the  $\nu_7$  mode of the acceptor. The donor absorption which is predicted to be shifted by  $25\text{--}35 \text{ cm}^{-1}$  to the blue could not be detected in the experiments. However, this is beyond the upper limit of the tuning range of the  $\text{CO}_2$  laser at  $1094 \text{ cm}^{-1}$ .

It is interesting to compare our results obtained using perturbation theory with quantum chemical calculations. Using MP2 methods, Ugliengo *et al.* find  $\nu_1$  band shifts of  $-80$  and  $+4 \text{ cm}^{-1}$  for the donor and the acceptor, respectively.<sup>23</sup> Here the agreement with experiments is clearly much better than for our perturbation calculations. This is, however, not the case for the CO stretching mode. Neglecting any mode couplings, Bizarri *et al.* find  $\nu_8$  band shifts of  $+12$  and  $-12 \text{ cm}^{-1}$  for the two molecules,<sup>74</sup> which is close to the findings of  $+12$  and  $-14 \text{ cm}^{-1}$  of the afore-

mentioned authors. The failure of these calculations to reproduce the asymmetry of the red and blue shift is probably caused by neglecting the cubic coupling to the  $\nu_1$  mode which is mostly responsible for the larger absolute shift of the donor vibrational mode.

For the cluster sizes from  $M=3$  to  $M=6$ , experimental spectra for size selected clusters are available only in the region of the  $\nu_8$  absorption. In contrast to the dimer spectra, only one band was recorded in the measured spectra of the trimer and the tetramer. In the present work this is explained by the existence of ring structures of  $C_{3h}$  symmetry for the trimer and  $C_{4h}$  symmetry for the tetramer. Only the doubly degenerate mode of  $E'$  and  $E_u$  symmetry, respectively, can be excited, while the other transitions are infrared forbidden. In principle, the occurrence of non-planar cluster geometries like the  $S_4$  structure which is obtained for the tetramer using the PHH3 potential can be ruled out merely by considering the number of spectral bands. However, the excitation of the  $B$  mode bears only very little infrared intensity and, therefore, might not be detected in an experiment. For the pentamer, the experimental spectrum again shows a single maximum. Omitting two modes of low infrared intensity, the theoretical spectra of the asymmetric ring structure consists of three absorption bands. However these are fairly close together. For example, using the PHH3 potential the calculated spacings of the absorption frequencies in the pentamer spectrum are below  $2\text{ cm}^{-1}$ . Therefore, it is likely that they cannot be resolved in an experiment using a line tunable  $\text{CO}_2$  laser with its typical resolution of  $1\text{--}2\text{ cm}^{-1}$ .

The interpretation of the spectrum of the methanol hexamer is especially interesting. Unlike the spectra of trimer, tetramer, and pentamer, the experimental spectrum exhibits a double peak structure with two blue shifted peaks of approximately the same intensity. Using the OPLS potential model four different classes of stable isomers were found. However, only the species of  $S_6$  symmetry has a spectrum with two absorption bands while all the other isomers show spectra with six peaks (see Fig. 6). Therefore, we can unambiguously conclude that in the molecular beam experiments only this ring-shaped isomer of  $S_6$  symmetry is present. The other six-membered ring structure of  $C_2$  symmetry as well as the other isomers consisting of branched rings can be clearly ruled out, although they are only slightly less stable. The interpretation of the double peak structures occurring in the dimer and in the hexamer spectrum is impressively supported by recent experiments of Buck and Hobein. Using a double resonance technique they showed that in both cases the two frequencies are indeed due to the absorption of only one isomeric species and are not caused by the coexistence of two (or more) isomers in the beam experiments.<sup>86</sup>

In a quantitative comparison of the band shifts the different properties of the two potential models (OPLS and PHH3) become obvious. For the dimer the calculated spectra of the  $\nu_8$  mode are in satisfactory agreement with the experimental results, especially the value of the line splitting of  $25\text{ cm}^{-1}$  is reproduced very well in both cases. The absolute values are slightly better for the PHH3 po-

tential, for which the calculated frequencies are  $5\text{--}6\text{ cm}^{-1}$  larger than the experimental ones, while this discrepancy is about  $10\text{ cm}^{-1}$  for the OPLS model. This difference may be caused by some apparent errors in the analytical forms of this model function, mainly the lack of a nonelectrostatic term for the O-H potential. These shortcomings of the potential models become more striking, when considering the band shifts of the OH stretching mode  $\nu_1$ . The red shift of the donor excitation is overestimated by 40% using the PHH3 potential while the results obtained for the OPLS potential differ by more than 100% from the experimental shifts. In addition, for the  $\nu_1$  vibration of the acceptor molecule the calculations are in error. The simulated  $\nu_7$  spectra, however, are in much better agreement with the experimental ones. The shift of the acceptor absorption of  $-3\text{ cm}^{-1}$  is reproduced well by the calculated values of  $-3.6$  and  $-2.1\text{ cm}^{-1}$  for the two potential models.

In the case of the trimer and the tetramer, however, there is no quantitative coincidence between our PHH3 calculations and the experimental results. For the trimer the predicted shift is completely in error ( $3\text{ cm}^{-1}$  vs  $64\text{ cm}^{-1}$ ). The failure of the PHH3 potential to reproduce the trimer spectrum is believed to be due to the rather steep increase of the potential terms which leads to too large effective force constants. For the tetramer with its  $S_4$  symmetry the blue shift of the  $E$  mode of  $+26.6\text{ cm}^{-1}$  is again much larger than the experimental shift of  $+10\text{ cm}^{-1}$ . The situation is slightly better for the OPLS potential. The tendency of an increasing blue shift from the trimer to the tetramer is in agreement with the experiments. However, the calculated step from the trimer shift of  $+3.8\text{ cm}^{-1}$  to the tetramer shift of  $+24.9\text{ cm}^{-1}$  is too large compared with the experimental step from  $+8$  to  $+10\text{ cm}^{-1}$ .

The theoretical spectra of the pentamer and the hexamer are again in much better agreement with the experimental ones. For the simulation of the pentamer using the PHH3 potential they coincide very well. The three absorptions at  $+14.7$ ,  $+16.6$ , and  $+16.9\text{ cm}^{-1}$  closely resemble the experimental spectrum with one broad band at  $+14\text{ cm}^{-1}$ . For the case of the hexamer with its bimodal spectrum the calculated splitting between the frequencies of the  $A_u$  and the  $E_u$  mode of  $16$  and  $13\text{ cm}^{-1}$  for the OPLS and PHH3 potential, respectively, are close to the experimental frequency splitting of  $12\text{ cm}^{-1}$ . As in the case of the dimer and pentamer the PHH3 potential model yields slightly better results for the absolute values of the blue shifts which are only  $4\text{--}5\text{ cm}^{-1}$  too large compared to the experimental shifts of  $+18\text{ cm}^{-1}$  and  $+6\text{ cm}^{-1}$ .

#### IV. SUMMARY

A method is presented to calculate shifts and splittings of vibrational bands in the infrared spectra of small homogeneous molecular clusters. It is based on degenerate perturbation theory up to second order and thus takes the coupling of the vibrations of the different molecules into account. The first order shift is interpreted as a direct change of the force constant,  $\partial^2 U / \partial q^2$ , while in second order each vibrational mode  $s$  contributes to the shift of the  $r$ th mode with the product of the cubic anharmonic cou-

pling constants  $\varphi_{rs}$  and the force  $-\partial U/\partial q_s$  acting on that mode. Therefore the complete intramolecular force field up to third order as well as the intermolecular interaction potential are necessary as input information.

The method is applied to calculate the excitation frequency of the OH stretching mode ( $\nu_1$ , 3681.5  $\text{cm}^{-1}$ ), the  $\text{CH}_3$  rocking mode ( $\nu_7$ , 1074.5  $\text{cm}^{-1}$ ) of the dimer and to the CO stretching mode ( $\nu_8$ , 1033.5  $\text{cm}^{-1}$ ) from the dimer to the hexamer. Using empirical potential models and calculated anharmonic force fields, frequency shifts are calculated and the results are compared with the experiments. They are able to explain the number and the assignment of the bands found in the measured spectra: (1) A site splitting for the dimer which is caused by the nonequivalent position of the donor and the acceptor molecule; (2) a single doubly degenerate excitation frequency for the planar ring structures of the trimer and the tetramer of  $C_{3h}$  symmetry; (3) three closely spaced lines for the slightly distorted ring of the pentamer, and (4) a doubly degenerate and a single frequency for the different coupling of the molecular vibrations in the cyclic isomer of the hexamer of  $S_6$  symmetry. A detailed analysis of the data shows that contributions of both first and second order are important and that the coupling of different vibrational modes which leads to delocalized vibrations is essential for the explanation of the data. Furthermore, the results are very sensitive to the model of the intermolecular potential surface.

The qualitative agreement of theoretical and calculated frequencies is very good. Moreover, in most cases our second order treatment also reproduces the experimental shifts quantitatively. However, there are still certain shortcomings for the methanol simulations. In particular, the calculated  $\nu_1$  band shifts of the dimer as well as the  $\nu_8$  band shifts of the trimer and tetramer are still not satisfactory. However, the results presented here are based on semi-empirical models of the intermolecular potential energy which were constructed to reproduce mainly bulk properties of methanol. Furthermore, it must not be overlooked that none of the potential parameters was fitted to spectroscopic data. In this context it would be very interesting to test a potential model which was published very recently by Anwender *et al.*<sup>87</sup> Using *ab initio* methods, they fitted potential functions for a full six-site model of the methanol molecule. Another important source of uncertainty is introduced by the intramolecular force fields used here. Especially the cubic constants describing the anharmonic coupling of the normal modes of vibration which are used to calculate the second order frequency shifts are still not very well known. Nonetheless it was shown for the example of small methanol clusters that this type of spectrum simulations can be a valuable help for the *interpretation* of vibrational predissociation spectra of weakly bound complexes. Our methods can also be used as a guideline for the experimentalist in *predicting* the number and approximate positions of absorption bands. Once the cubic force fields are established more precisely, the perturbational methods presented here may also be used to improve the modeling of potential energy hypersurfaces and provide an ideal means of investigating the nature of intermolecular forces.

## ACKNOWLEDGMENTS

We would like to thank Professor R. O. Watts for many helpful discussions and for providing us a computer code for the calculation of second virial coefficients. One of us (B. S.) also thanks him for his great hospitality during a visit at the University of Washington. Financial support from Sonderforschungsbereich 93 and Schwerpunktprogramm "Molekulare Cluster" of the Deutsche Forschungsgemeinschaft is gratefully acknowledged.

- <sup>1</sup>A. C. Legon and D. J. Miller, *Chem. Rev.* **86**, 635 (1986).
- <sup>2</sup>D. J. Nesbitt, *Chem. Rev.* **88**, 843 (1988).
- <sup>3</sup>J. R. Heath, R. A. Sheekes, A. L. Crosky, and R. J. Saycally, *Science* **249**, 855 (1990).
- <sup>4</sup>T. E. Gough, R. E. Miller, and G. Scoles, *J. Chem. Phys.* **69**, 1588 (1978).
- <sup>5</sup>R. E. Miller, *Science* **240**, 447 (1988).
- <sup>6</sup>U. Buck and H. Meyer, *Phys. Rev. Lett.* **52**, 109 (1984); *J. Chem. Phys.* **84**, 4854 (1986).
- <sup>7</sup>U. Buck, *J. Phys. Chem.* **92**, 1023 (1988).
- <sup>8</sup>U. Buck, *Ber. Bunsenges. Phys. Chem.* **96**, 1275 (1992); U. Buck and I. Ettischer (unpublished).
- <sup>9</sup>U. Buck, F. Huisken, Ch. Lauenstein, H. Meyer, and R. Sroka, *J. Chem. Phys.* **87**, 6276 (1987).
- <sup>10</sup>F. Huisken and T. Pertsch, *J. Chem. Phys.* **86**, 106 (1987).
- <sup>11</sup>F. Huisken and M. Stemmler, *Chem. Phys. Lett.* **132**, 351 (1989).
- <sup>12</sup>A. deMeijere and F. Huisken, *J. Chem. Phys.* **92**, 5826 (1990).
- <sup>13</sup>U. Buck, X. J. Gu, R. Krohne, and Ch. Lauenstein, *Chem. Phys. Lett.* **174**, 247 (1990).
- <sup>14</sup>(a) U. Buck, X. J. Gu, Ch. Lauenstein, and A. Rudolph, *J. Phys. Chem.* **92**, 5561 (1988); (b) *J. Chem. Phys.* **92**, 6017 (1990).
- <sup>15</sup>F. Huisken and M. Stemmler, *Chem. Phys. Lett.* **144**, 391 (1988).
- <sup>16</sup>J. LaCosse and J. M. Lisy, *J. Phys. Chem.* **94**, 4398 (1990).
- <sup>17</sup>F. Huisken, A. Kulcke, C. Laush, and J. M. Lisy, *J. Chem. Phys.* **95**, 3924 (1991).
- <sup>18</sup>F. Huisken and M. Stemmler, *Z. Phys. D* **24**, 277 (1992).
- <sup>19</sup>F. Huisken and T. Pertsch, *Chem. Phys.* **126**, 213 (1988).
- <sup>20</sup>U. Buck, X. J. Gu, M. Hobein, and Ch. Lauenstein, *Chem. Phys. Lett.* **163**, 455 (1988).
- <sup>21</sup>U. Buck, X. J. Gu, R. Krohne, Ch. Lauenstein, H. Linnartz, and A. Rudolph, *J. Chem. Phys.* **94**, 23 (1991).
- <sup>22</sup>K. P. Sagarik, R. Ahlrichs, and S. Brode, *Mol. Phys.* **57**, 1247 (1986).
- <sup>23</sup>P. Ugliengo, A. Bleiber, E. Garrone, J. Sauer, and A. M. Ferrari, *Chem. Phys. Lett.* **191**, 537 (1992).
- <sup>24</sup>I. A. Mills, in *Molecular Spectroscopy: Modern Research*, edited by K. N. Rao and C. W. Mathews (Academic, New York, 1972), p. 115.
- <sup>25</sup>A. D. Buckingham, *Proc. R. Soc. London, Ser. A* **248**, 169 (1958).
- <sup>26</sup>A. D. Buckingham, *Proc. R. Soc. London, Ser. A* **255**, 32 (1960).
- <sup>27</sup>A. D. Buckingham, *Trans. Faraday Soc.* **56**, 753 (1960).
- <sup>28</sup>E. Shalev, N. Ben-Horin, U. Even, and J. Jortner, *J. Chem. Phys.* **95**, 3147 (1991).
- <sup>29</sup>M. R. Zakin and D. R. Herschbach, *J. Chem. Phys.* **85**, 2376 (1986).
- <sup>30</sup>H. Friedmann and S. Kimel, *J. Chem. Phys.* **43**, 3925 (1965).
- <sup>31</sup>A. S. Al-Mubarak, G. Del Mistro, P. G. Lethbridge, N. Y. Abdulsattar, and A. J. Stace, *Trans. Faraday Soc.* **86**, 209 (1988).
- <sup>32</sup>U. Buck and B. Schmidt, *J. Mol. Liq.* **46**, 181 (1990).
- <sup>33</sup>M. Snels and R. Fantoni, *Chem. Phys.* **109**, 67 (1986).
- <sup>34</sup>M. Snels and J. Reuss, *Chem. Phys. Lett.* **140**, 543 (1987).
- <sup>35</sup>J. Geraedts, S. Stolte, and J. Reuss, *Z. Phys. A* **304**, 167 (1982).
- <sup>36</sup>J. Geraedts, M. Waayer, S. Stolte, and J. Reuss, *Faraday Discuss. Chem. Soc.* **73**, 375 (1982).
- <sup>37</sup>J. A. Barnes and T. E. Gough, *J. Chem. Phys.* **86**, 6012 (1987).
- <sup>38</sup>G. Cardini, V. Schettino, and M. L. Klein, *J. Chem. Phys.* **90**, 4441 (1989).
- <sup>39</sup>D. Eichenauer and R. J. Le Roy, *J. Chem. Phys.* **88**, 2898 (1988).
- <sup>40</sup>M. A. Kmetc and R. J. Le Roy, *J. Chem. Phys.* **95**, 6271 (1991).
- <sup>41</sup>J. W. I. van Bladel and A. van der Avoird, *J. Chem. Phys.* **92**, 2837 (1990).
- <sup>42</sup>M. F. Vernon, D. J. Krajnovich, H. S. Kwok, J. M. Lisy, Y. R. Shen, and Y. T. Lee, *J. Chem. Phys.* **77**, 47 (1982).

- <sup>43</sup>D. F. Coker, R. E. Miller, and R. O. Watts, *J. Chem. Phys.* **82**, 3554 (1985).
- <sup>44</sup>E. Honegger and S. Leutwyler, *J. Chem. Phys.* **88**, 2582 (1988).
- <sup>45</sup>F. Huisken and M. Stemmler, *Chem. Phys. Lett.* **180**, 332 (1991).
- <sup>46</sup>A. Dalgarno, in *Quantum Theory*, edited by D. R. Bates (Academic, New York, 1961), p. 171.
- <sup>47</sup>A. R. Hoy, I. M. Mills, and G. Strey, *Mol. Phys.* **24**, 1265 (1972).
- <sup>48</sup>J. A. Beswick, in *Structure and Dynamics of Weakly Bound Complexes*, edited by A. Weber (Reidel, Dordrecht, 1987), p. 563.
- <sup>49</sup>R. J. LeRoy, M. R. Davies, and M. E. Lam, *J. Phys. Chem.* **95**, 2167 (1990).
- <sup>50</sup>U. Buck, M. Hobein, and B. Schmidt, *J. Chem. Phys.* **98**, 9425 (1993).
- <sup>51</sup>P.-O. Westlund and R. M. Lynden-Bell, *Mol. Phys.* **60**, 1189 (1987).
- <sup>52</sup>J. G. Powles, S. Murad, D. P. Sethi, and P. V. Ravi, *Mol. Phys.* **73**, 1307 (1991).
- <sup>53</sup>A. M. Benson and H. G. Drickamer, *J. Chem. Phys.* **27**, 1164 (1957).
- <sup>54</sup>U. Buck, B. Schmidt, and J. Siebers (unpublished).
- <sup>55</sup>J. C. G. M. van Duijneveldt-van de Rijdt, and F. B. van Duijneveldt, *J. Comput. Chem.* **13**, 399 (1992).
- <sup>56</sup>F. G. Dijkman and J. H. van der Maas, *J. Chem. Phys.* **66**, 3871 (1977).
- <sup>57</sup>R. O. Watts, in *The Chemical Physics of Atomic and Molecular Clusters*, edited by G. Scoles (North-Holland, Amsterdam, 1990), p. 271.
- <sup>58</sup>R. E. Miller, R. O. Watts, and A. Ding, *Chem. Phys.* **83**, 155 (1984).
- <sup>59</sup>J. C. Decius, *J. Chem. Phys.* **49**, 1387 (1968).
- <sup>60</sup>J. M. Hutson, *J. Chem. Phys.* **96**, 6752 (1992); *J. Phys. Chem.* **96**, 4237 (1992).
- <sup>61</sup>S.-Y. Liu and C. E. Dykstra, *J. Phys. Chem.* **90**, 3097 (1986).
- <sup>62</sup>J. Detrich, G. Corongiu, and E. Clementi, *Chem. Phys. Lett.* **112**, 426 (1984).
- <sup>63</sup>W. L. Jorgensen, *J. Phys. Chem.* **90**, 1276 (1986).
- <sup>64</sup>G. Pálincás, E. Hawlicka, and K. Heinzinger, *J. Phys. Chem.* **91**, 4334 (1987).
- <sup>65</sup>1 Debye =  $3.3356 \times 10^{-30}$  Cm.
- <sup>66</sup>T. E. Gough, X. J. Gu, N. R. Isenor, and G. Scoles, *Int. J. Infrared Millimeter Wave* **7**, 1893 (1986).
- <sup>67</sup>J. Snir, R. A. Nemenoff, and H. A. Scheraga, *J. Phys. Chem.* **82**, 2497 (1978).
- <sup>68</sup>F. T. Marchese, P. K. Mehrota, and D. L. Beveridge, *J. Phys. Chem.* **86**, 2592 (1982).
- <sup>69</sup>D. J. Evans and R. O. Watts, *Mol. Phys.* **28**, 1233 (1974).
- <sup>70</sup>D. J. Evans, in *Computational Methods in Mathematical Physics*, edited by R. S. Anderssen and R. O. Watts (Queensland University, Melbourne, 1975).
- <sup>71</sup>J. H. Dymond and E. B. Smith, *The Virial Coefficients of Pure Gases and Mixtures* (Oxford University, London, 1980).
- <sup>72</sup>The quasi-Newton algorithm used in the multidimensional minimization was EO4JAF from the NAG library.
- <sup>73</sup>L. A. Curtiss, *J. Chem. Phys.* **67**, 1144 (1977).
- <sup>74</sup>A. Bizarri, S. Stolte, J. Reuss, J. C. G. M. van Duijneveldt-van de Rijdt, and F. B. van Duijneveldt, *Chem. Phys.* **143**, 423 (1990).
- <sup>75</sup>T. A. Renner, G. H. Kucera, and M. Blander, *J. Chem. Phys.* **66**, 177 (1977).
- <sup>76</sup>L. A. Curtiss and M. Blander, *Chem. Rev.* **88**, 827 (1988).
- <sup>77</sup>T. P. Martin, T. Bergmann, and B. Wassermann, in *Large Finite Systems*, edited by J. Jortner and B. Pullmann (Reidel, Dordrecht, 1987).
- <sup>78</sup>G. Brink and L. Glasser, *J. Comput. Chem.* **2**, 14 (1981).
- <sup>79</sup>J. A. Odutola, R. Viswanathan, and T. R. Dyke, *J. Am. Chem. Soc.* **101**, 4787 (1979).
- <sup>80</sup>K.-P. Schröder, *Chem. Phys.* **123**, 91 (1988).
- <sup>81</sup>B. J. Mhin, H. S. Kim, H. S. Kim, C. W. Yoon, and K. S. Kim, *Chem. Phys. Lett.* **176**, 41 (1991).
- <sup>82</sup>H. B. Schlegel, S. Wolfe, and F. Bernardi, *J. Chem. Phys.* **67**, 4181 (1977). Additional tables with calculated anharmonic force constants, harmonic frequencies, and anharmonicity constants are published in AIP document No. PAPS JCPSA 67-4181-13.
- <sup>83</sup>P. Botschwina and W. Meyer, *Chem. Phys.* **15**, 25 (1976).
- <sup>84</sup>A. Serrallach, R. Meyer, and H. H. Günthard, *J. Mol. Spectrosc.* **52**, 94 (1974).
- <sup>85</sup>G. Kabisch and M. Pollmer, *J. Mol. Struct.* **81**, 35 (1982).
- <sup>86</sup>U. Buck and M. Hobein (unpublished).
- <sup>87</sup>E. H. S. Anwander, M. M. Probst, and B. M. Rode, *Chem. Phys.* **166**, 341 (1992).